

pubs.acs.org/JPCL Letter

# Magic Angle Spinning Solid-State <sup>13</sup>C Photochemically Induced Dynamic Nuclear Polarization by a Synthetic Donor-Chromophore-Acceptor System at 9.4 T

Federico De Biasi, Michael A. Hope, Yunfan Qiu, Paige J. Brown, Máté Visegrádi, Olivier Ouari, Michael R. Wasielewski, and Lyndon Emsley\*



Cite This: J. Phys. Chem. Lett. 2024, 15, 5488-5494



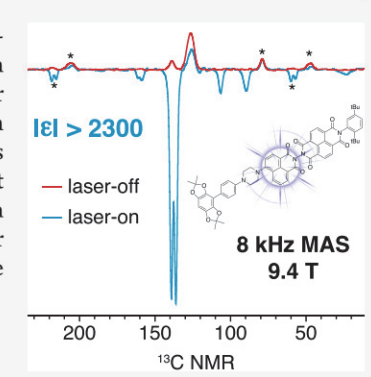
ACCESS I

III Metrics & More

Article Recommendations

Supporting Information

ABSTRACT: Solid-state photochemically induced dynamic nuclear polarization (photo-CIDNP) is a nuclear magnetic resonance spectroscopy technique in which nuclear spin hyperpolarization is generated upon optical irradiation of an appropriate donor-acceptor system. Until now, solid-state photo-CIDNP at high magnetic fields has been observed only in photosynthetic reaction centers and flavoproteins. In the present work, we show that the effect is not limited to such biomolecular samples, and solid-state <sup>13</sup>C photo-CIDNP can be observed at 9.4 T under magic angle spinning using a frozen solution of a synthetic molecular system dissolved in an organic solvent. Signal enhancements for the source molecule larger than a factor of 2300 are obtained. In addition, we show that bulk <sup>13</sup>C hyperpolarization of the solvent can be generated via spontaneous <sup>13</sup>C-<sup>13</sup>C spin diffusion at natural abundance.



uclear magnetic resonance (NMR) spectroscopy is an indispensable tool (see the control of the co indispensable tool for chemical and structural analysis owing to its outstanding ability to capture changes in the local environment at the atomic scale. Nonetheless, the flip side of NMR lies in its low sensitivity compared to other spectroscopic methods, where reduced sensitivity is a direct outcome of the small energy gap that separates the nuclear spin states, resulting in only a minor population imbalance, even at liquid nitrogen temperatures (80-100 K).<sup>1,2</sup>

To combat the low sensitivity of NMR, several methods have been designed to enhance the spin population imbalance beyond the thermal equilibrium, generating so-called hyperpolarization.<sup>3-9</sup> These hyperpolarization methods in NMR spectroscopy boost the sensitivity of the technique by orders of magnitude, allowing complex analyses to be performed, which would otherwise not be possible. 3,10 In the solid state, the most widespread NMR hyperpolarization protocol is dynamic nuclear polarization (DNP), 11,12 where, upon microwave irradiation, thermal electron spin polarization is transferred from a paramagnetic species to neighboring nuclei, typically <sup>1</sup>H spins, and then is relayed to the bulk of the sample by spontaneous spin diffusion. 13,14

The signal enhancement  $(\varepsilon)$  provided by DNP is limited, among other factors, by the magnitude of the thermal electron spin polarization and cannot theoretically exceed a factor of 658 for <sup>1</sup>H nuclei or 2610 for <sup>13</sup>C nuclei ( $\epsilon_{\rm DNP}^{\rm max} = |\gamma_{\rm e}/\gamma_{\rm N}|$ , where  $\gamma_{\rm e}$  and  $\gamma_{\rm N}$  are the electron and nuclear gyromagnetic ratios).<sup>2</sup> On the other hand, optically induced NMR hyperpolarization methods exploit transient excited states as the initial source of polarization. Such excited states can be characterized by a non-Boltzmann spin population imbalance; therefore, they can provide nuclear hyperpolarization exceeding the DNP limit,

One optical NMR hyperpolarization protocol is photochemically induced dynamic nuclear polarization (photo-CIDNP). 21-25 In the solid state, photo-CIDNP is observed in donor-acceptor systems that undergo charge separation upon irradiation with light, generating a transient spincorrelated radical pair (SCRP).26 The SCRP is typically generated in the singlet state, IS>. At high fields, the SCRP coherently evolves between the singlet and the  $|T_0\rangle$  triplet state, potentially accumulating nuclear hyperpolarization during the process. 22,27,28 Until now, solid-state photo-CIDNP at magnetic fields larger than 1 T has been investigated only in flavoproteins and photosynthetic reaction centers, where solely <sup>13</sup>C and <sup>15</sup>N nuclei have been directly polarized. <sup>26,29–44</sup> Recently, we reported the first example of direct <sup>1</sup>H photo-CIDNP in solids, at 0.3 T, using a synthetic donor-chromophore-acceptor (D-C-A) molecular system dissolved in a glassy frozen matrix. 45 In this study, <sup>1</sup>H-<sup>1</sup>H spin

Received: April 16, 2024 Revised: May 6, 2024 Accepted: May 10, 2024 Published: May 15, 2024





diffusion was exploited to relay the polarization from the D–C–A system to the glassy matrix, leading to bulk uniform polarization of the sample. This was in contrast with most solid-state photo-CIDNP studies on photosensitive proteins, where the poor spin diffusion efficiency of <sup>13</sup>C and <sup>15</sup>N nuclei at natural abundance confines the polarization in the vicinity of the donor–acceptor system.

Here, we extend the concept of solid-state photo-CIDNP hyperpolarization by a D–C–A molecule to the high magnetic fields required for high-resolution NMR (here, 9.4 T). The advantages of small molecules over biomolecular systems, such as flavoproteins and photosynthetic reaction centers, are the easier tuneability of the photoactive machinery and broader solvent compatibility. However, to the best of our knowledge, no solid-state photo-CIDNP activity has been reported on D–C–A molecular systems at fields >1 T.

In the present work, we show that solid-state <sup>13</sup>C photo-CIDNP can occur in a D-C-A molecule in a frozen solution at 9.4 T, where D is benzobisdioxole aniline (BDX), C is 4-aminonaphthalene-1,8-dicarboximide (ANI), and A is naphthalene-1,8:4,5-bis(dicarboximide) (NDI). We refer to this motif as CarboPol. The structure of CarboPol is shown in Figure 1, together with its photocycle. Upon absorption of a

**Figure 1.** (a) Structure of the CarboPol molecule introduced in this work. The donor (BDX), chromophore (ANI), and acceptor (NDI) in the photoactive part of the structure are shown in red, yellow, and blue, respectively. The linker and end group are shown in black. (b) Photocycle of the D–C–A system in CarboPol ( $h\nu$ , photoexcitation; ISC, intersystem crossing; and CR, charge recombination).

photon by the chromophore, an excited state  $D-C^*-A$  is populated, which then undergoes an intramolecular electron transfer to form a charge-separated state. This charge-separated state is a singlet-born SCRP, indicated as  $^1(D^{+\bullet}-C-A^{-\bullet})$  in Figure 1. The radical pair then evolves between that and the  $|T_0\rangle$  state, denoted as  $^3(D^{+\bullet}-C-A^{-\bullet})$ , and eventually decays to either the initial state or the neutral triplet state via charge recombination (CR). In the case of CarboPol, the neutral triplet that is created after CR in the triplet channel ( $^3$ CR) is localized on the acceptor and has the form  $D-C^{-3}A$ .

CarboPol was synthesized as detailed in the Supporting Information. The molecule was designed on the basis of an established family of very well-characterized D–C–A molecules. <sup>46–56</sup> It shares features with the previously introduced PhotoPol molecule that showed a <sup>1</sup>H photo-CIDNP response at 0.3 T. <sup>45</sup> CarboPol was designed to have a stronger electron–electron coupling as a result of the shorter donor–acceptor distance

For all of the NMR experiments presented here, o-terphenyl (OTP) was used as a glassy matrix for its favorable solvation and glass-forming properties, optical transparency, and long nuclear spin longitudinal relaxation times.<sup>57-60</sup> <sup>13</sup>C photo-CIDNP experiments were carried out at 9.4 T (100.6 MHz <sup>13</sup>C Larmor frequency) and cryogenic temperatures (100-220 K) using an Avance III HD Bruker NMR spectrometer and a commercial low-temperature magic angle spinning (MAS) DNP probe, in which a portion of the microwave waveguide was modified to allow for optical irradiation of the spinning sample (Figures S1-S3 of the Supporting Information). Samples were packed in a 3.2 mm sapphire rotor to allow for light penetration and sealed with a silicone plug. The MAS rate was 8 kHz in all of the experiments. Sample irradiation was achieved with a continuous wave 450 nm blue laser (the laser output power is 1.3 W, but the power delivered to the sample is likely to be significantly lower). In the laser-on experiments, the laser was on for the whole duration of the experiments. Experiments at 0.3 T were performed as described previously, 45 using a laser intensity of 4.2 W cm<sup>-2</sup>.

First, we note that CarboPol shows solid-state  $^1H$  photo-CIDNP activity at 0.3 T (Figure S13 of the Supporting Information), giving a bulk  $^1H$  signal enhancement factor of  $\varepsilon_{1H}^{\text{bulk}} = -27$  at a 20 s recycle delay ( $\varepsilon = I_{\text{on}}/I_{\text{off}}$ ). This bulk enhancement factor is 1.7 times larger than that previously observed with PhotoPol under similar conditions. CarboPol has a larger electron–electron coupling compared to that of PhotoPol ( $d \approx -60$  MHz versus -5.5 MHz), as measured in butyronitrile at 85 K (details in the Supporting Information). This larger coupling could enable three-spin mixing at higher fields.  $^{27,28}$ 

Figure 2 shows the direct excitation <sup>13</sup>C NMR spectra of a 1.5 mM frozen solution of CarboPol in OTP at 9.4 T and 100 K with (blue) and without (red) 450 nm laser irradiation, using a recycle delay of 1.8 s. In the absence of irradiation, only the OTP solvent signal is detected. With light irradiation, the <sup>13</sup>C signals of the CarboPol molecule can clearly be observed. Interestingly, all of the <sup>13</sup>C photo-CIDNP signals are negatively enhanced, irrespective of whether they belong to the donor or acceptor part of the photoactive machinery. A tentative assignment is also shown based on <sup>13</sup>C chemical shifts and solution-state NMR data (Figures S4-S7 of the Supporting Information). Note that the large signal from the silicone plug is due to its short <sup>13</sup>C T<sub>1</sub> compared to OTP, given the short experimental recycle delay. The reduction of the OTP signal at 126 ppm in the laser-on spectrum could be due to an overlap with negatively enhanced 13C signals of the NDI acceptor (Figure S5 of the Supporting Information).

Because the CarboPol signal without irradiation is too weak to be observed at 1.5 mM with 30 000 scans (15 h), it is not possible to determine the enhancement factor directly. Using the noise level in the laser-off spectrum, we can obtain a lower bound for the magnitude of the  $^{13}$ C enhancement factor for the signals at 138 ppm (corresponding to four of the aromatic sites in the BDX donor) of  $|\varepsilon_{13C}| > |-340| = 340$  at a 1.8 s

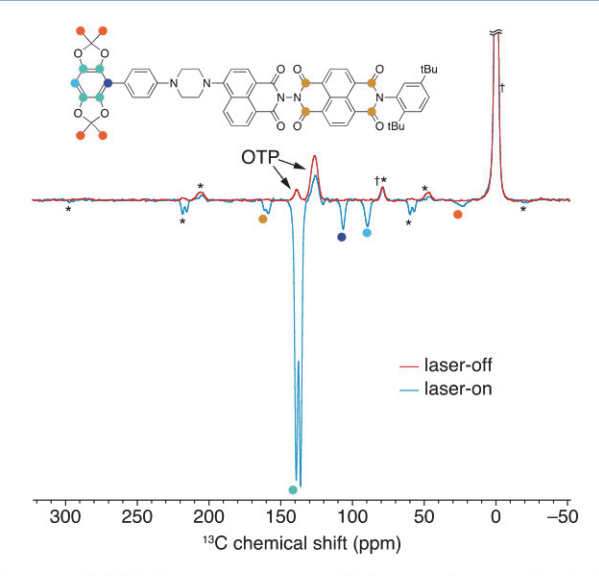


**Figure 2.** <sup>13</sup>C NMR spectra of a 1.5 mM frozen solution of CarboPol in OTP (9.4 T, 8 kHz MAS, and 100 K) without (red) and with (blue) continuous wave 450 nm laser irradiation. The recycle delay ( $\tau$ ) was set equal to the polarization build-up time under laser irradiation ( $T_{\rm b}=1.8$  s; data shown below), and an excitation pulse of 68° was used to maximize the signal-to-noise ratio per unit time in the laser-on spectrum (Ernst angle for  $\tau=T_{\rm b}$ ). <sup>61</sup> Both spectra were acquired with 30 000 scans. The asterisks indicate spinning sidebands, while the daggers denote the silicone plug signals. The colored circles on the spectrum and on the molecular structure shown in the inset indicate the assignment of the photo-CIDNP-enhanced signals (the complete assignment in solution is shown in the Supporting Information).

recycle delay ( $\varepsilon = I_{\rm on}/N_{\rm off}$ ) with I and N being the signal intensity and the noise level). To obtain a higher sensitivity laser-off spectrum, we repeated the same laser-off experiment on two separate 15 mM CarboPol samples in OTP, i.e., 10 times more concentrated than the sample used to acquire the spectra in Figure 2. Further details are given in the Supporting Information. Even at 15 mM, no CarboPol aromatic signals were observed without laser irradiation after 30 000 scans (Figures S8–S10 of the Supporting Information). This led to an improved estimate of the enhancement factor of the signals at 138 ppm at a 1.8 s recycle delays of  $|\varepsilon_{\rm 13C}| > 2300$ .

Degradation of the 1.5 mM CarboPol sample was also investigated during a 10 h period of continuous 450 nm laser irradiation at 100 K. Figure 3 reports the normalized integrated intensity of the BDX donor aromatic signals at 138 ppm as a function of time. After 10 h, the peak area was reduced only by 3%, suggesting that degradation of the sample as a result of laser irradiation is very slow under MAS at this temperature. Therefore, long experiments on this and similar systems are, in principle, feasible, without significant loss in quality over time of the recorded NMR signal.

The effect of the temperature on the <sup>13</sup>C photo-CIDNP activity in CarboPol has also been investigated with a 1.8 s recycle delay within the 100–220 K range, below the glass transition temperature of OTP (243 K). <sup>57</sup> The magnitude of the <sup>13</sup>C photo-CIDNP-enhanced signals decreases with an increasing temperature, as shown in Figure 4. The effect is likely due to a shorter SCRP lifetime at higher temperatures, but other parameters (e.g., the electron–electron coupling d) might depend upon the temperature as well, affecting the photo-CIDNP activity. The increasing magnitude of the OTP

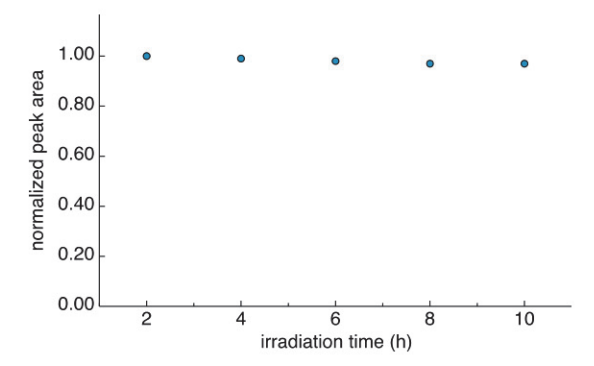


**Figure 3.** Intensity of the photo-CIDNP effect in CarboPol as a function of the irradiation time with a continuous wave 450 nm laser. Each data point corresponds to the area of the BDX donor aromatic peak at 138 ppm in a direct excitation NMR experiment, each acquired over a 2 h period using an interscan delay of 1.8 s and an excitation pulse of  $68^{\circ}$  (3972 scans per data point). Data are normalized by the signal area in the spectrum after the first 2 h. Error bars are smaller than the symbol size.

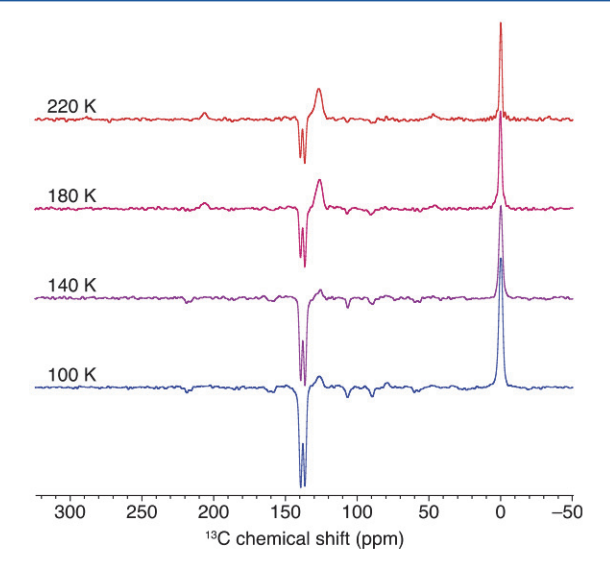


**Figure 4.** <sup>13</sup>C NMR spectra of a 1.5 mM frozen solution of CarboPol in OTP (9.4 T, 8 kHz MAS) in the presence of 450 nm laser irradiation. Spectra were collected at the indicated temperatures from colder to warmer using a 1.8 s recycle delay, 2000 scans, and an excitation pulse of 68°.

signal at 126 ppm with the temperature is ascribed to either faster  $^{13}$ C  $T_1$  relaxation for OTP at higher temperatures or a reduction of the negative photo-CIDNP effect for the CarboPol resonances underneath the OTP signal (especially those from the carbons of the NDI acceptor; Figure S5 of the Supporting Information) or to a combination of the two effects. No sample degradation occurred during the acquisition of the spectra in Figure 4, as suggested by the full recovery of the photo-CIDNP effect when the sample was cooled down again to 100 K (Figure S11 of the Supporting Information).

The polarization build-up with laser irradiation of the CarboPol signals at 138 ppm was characterized on the same sample (1.5 mM CarboPol in OTP) at 100 K and 8 kHz MAS. Results are shown in Figure 5. Data were fit to a biexponential function  $I(t) = I_{\rm fast}(1 - {\rm e}^{-t/T_{\rm b,fast}}) + I_{\rm slow}(1 - {\rm e}^{-t/T_{\rm b,slow}})$ , where the fast component corresponds to the BDX donor aromatic signals and the slow component corresponds to the over-

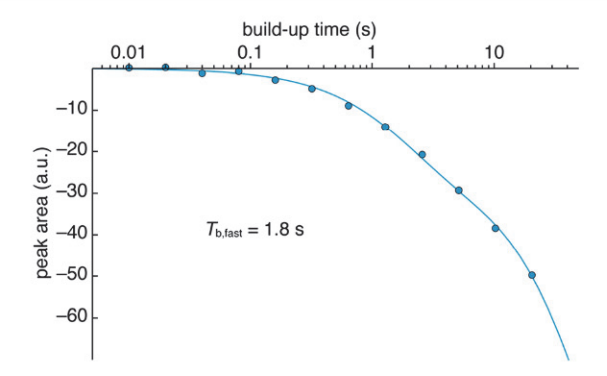


**Figure 5.** Polarization build-up at 100 K in the presence of continuous wave 450 nm laser irradiation of the CarboPol aromatic signals at 138 ppm (from the BDX donor). The solid blue line shows the best fit to a biexponential function (see the main text for details). Error bars for each data point have a comparable size to the symbols and have been omitted.

lapping OTP signal. The characteristic build-up time of the photo-CIDNP-enhanced signal was estimated to be 1.8 s. The characteristic build-up time of OTP was not accurately determined here as a result of the long experimental time that would be required.

From the build-up curve in Figure 5, it is evident that, for longer recycle delays, the overlapping OTP solvent signal also becomes negatively enhanced, as the overall integrated intensity of the signals at 138 ppm continues to decrease even at times longer than  $5T_{b,fast}$ . This can be seen directly from the other OTP peak at 126 ppm, which becomes negative in the laser-on spectrum with a recycle delay of 20 s (Figure S12 of the Supporting Information). This evidence demonstrates that the <sup>13</sup>C polarization propagates from the CarboPol molecules to the OTP solvent molecules in the bulk of the sample via spontaneous <sup>13</sup>C-<sup>13</sup>C spin diffusion, despite the very low efficiency of the process (all compounds here are at natural <sup>13</sup>C abundance). Indeed, <sup>13</sup>C-<sup>13</sup>C spin diffusion can still occur because of the very long  $^{13}$ C  $T_1$  of OTP, which is expected to be on the order of 1000 s at 100 K. Assuming that the spin diffusion coefficient (D) is proportional to  $\gamma_N^2 c^{1/3}$ , where c is the concentration of the nuclear spins (0.86 M for <sup>13</sup>C in pure OTP), we can estimate its value for <sup>13</sup>C spins in bulk OTP to be  $D = 11 \text{ nm}^2 \text{ s}^{-1}$  by rescaling the measured spin diffusion coefficient of <sup>19</sup>F in CaF<sub>2</sub> || [001].<sup>62</sup> Considering a  $^{13}$ C  $T_1$  of 1000 s, the  $^{13}$ C spin diffusion length, defined as  $\lambda =$  $\sqrt{DT_1}$ , is approximatively 100 nm. This analysis does not account for the influence of MAS on D,63 which could significantly reduce the value of  $\lambda$  for dilute and low- $\gamma$  spins because of the reduced homonuclear dipolar interaction. Nevertheless, to explore the extent of bulk 13C polarization that can be generated at 100 K via <sup>13</sup>C-<sup>13</sup>C spin diffusion from the CarboPol molecules in this formulation, we measured two spectra with a long recycle delay of 2 h (Figure 6). Without light (red), conventional  $T_1$  relaxation restores the OTP polarization to its thermal equilibrium, while in the presence of light (blue), the large negative 13C polarization is relayed via spin diffusion from CarboPol, which now effectively acts as a polarizing agent, to the bulk of the sample. The <sup>13</sup>C bulk enhancement at a 2 h recycle delay under 8 kHz MAS is  $\varepsilon_{13C}^{\text{bulk}}$  = -4.7 ( $\varepsilon = I_{\rm on}/I_{\rm off}$ ). Note that the signal from the silicone plug is not enhanced and, with this long recycle delay, is now dwarfed by the OTP signal. The large difference between the

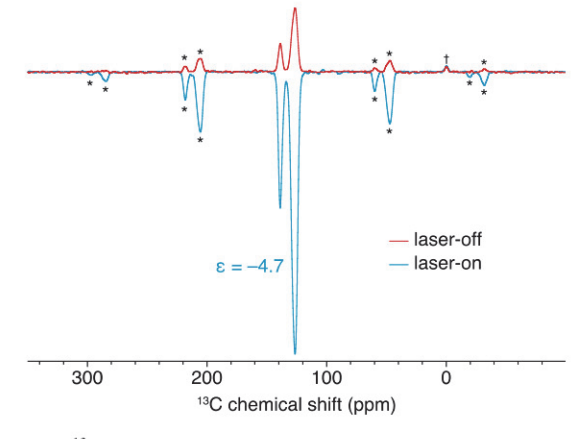


**Figure 6.** <sup>13</sup>C NMR spectra of a 1.5 mM frozen solution of CarboPol in OTP (9.4 T, 8 kHz MAS, and 100 K) without (red) and with (blue) laser irradiation (2 h recycle delay and 90° excitation pulse). Both spectra were acquired with four scans. The asterisks indicate spinning sidebands, while the dagger denotes the silicone plug signal.

high local enhancements on CarboPol and the modest OTP bulk enhancement is ascribed to the very limited  $^{13}C-^{13}C$  spin diffusion efficiency.  $^{64}$ 

We now consider the photo-CIDNP mechanism at play here. The simplest Hamiltonian used to describe high-field photo-CIDNP of a single nuclear spin can be expressed as<sup>28</sup>

$$\hat{H} = \omega_{1e}\hat{S}_{1z} + \omega_{2e}\hat{S}_{2z} + \omega_{N}\hat{I}_{z} + \frac{d}{2}(\hat{S}_{1+}\hat{S}_{2-} + \hat{S}_{1-}\hat{S}_{2+})$$

$$+ a\hat{S}_{1z}\hat{I}_{z} + b\hat{S}_{1z}\hat{I}_{x}$$

where  $\omega_{1\rm e}$  and  $\omega_{2\rm e}$  are the electron spin Larmor frequencies of the SCRP,  $\omega_{\rm N}$  is the nuclear spin Larmor frequency, d is the electron–electron interaction strength, and a and b are the secular and pseudo-secular components of the hyperfine interaction (coupling with only one electron of the SCRP is assumed). Solid-state photo-CIDNP generates nuclear hyperpolarization according to three different mechanisms: differential relaxation (DR),  $^{30,65}$  differential decay (DD),  $^{41}$  and three-spin mixing (TSM).  $^{66,67}$  These mechanisms are not mutually exclusive and could act simultaneously;  $^{27,28}$  however, the values of the spin interactions in CarboPol and the sign of the photo-CIDNP enhancement allow us to determine which mechanism dominates.

DR is most efficient when  $|\Delta\omega_{\rm e}| = |\omega_{1\rm e} - \omega_{2\rm e}| = |a/2|$ , while DD is most efficient when  $|\omega_{\rm N}| = |a/2|$ . TSM can occur under two different regimes: a first regime involving a double matching condition of the form  $|\Delta\omega_{\rm e}| = |\omega_{\rm N}| = |a/2|$  and a second regime occurring when  $|\omega_{\rm N}| = \sqrt{d^2 + a^2/4}$ . <sup>27,28,66–68</sup>

On the basis of the calculated g-factors of the BDX and NDI cationic and anionic radicals in CarboPol, <sup>46</sup>  $|\Delta\omega_e|$  at 9.4 T is expected to be between 100 and 300 MHz for most molecular orientations. At the same time,  $|\omega_N|$  for <sup>13</sup>C nuclei at 9.4 T is 100.6 MHz. Therefore, for maximum efficiency, both DR and DD require hyperfine couplings on the <sup>13</sup>C sites in CarboPol on the order of a few hundred MHz, which is unrealistic for this system. <sup>46</sup> On the other hand, the relative sizes of  $\omega_N$  and d ( $\omega_N = -100.6$  MHz and  $d \approx -60$  MHz; details in the Supporting Information) suggest that TSM can still occur in a regime for which the matching condition is approximatively satisfied ( $|\omega_N| \approx |d|$ ). Indeed, we designed CarboPol to have a short donor–acceptor distance for which the electron–

electron coupling is dominated by a scalar interaction on the order of 100 MHz. The sign of the signal enhancement via the TSM mechanism only depends upon the sign of d and is expected to be negative for both the donor and acceptor sites, which is indeed the case. This also adds weight to the hypothesis that TSM dominates over DR and DD, as the acceptor signal would dominate for DR, while for DD, both positive and negative enhancements would be expected.  $^{28,30,41,46,65}$ 

In conclusion, we have shown that solid-state <sup>13</sup>C photo-CIDNP can be observed in synthetic donor—acceptor systems at a high magnetic field, if the electronic properties can be designed to match the photo-CIDNP conditions. The effect was proven to be active at 9.4 T and up to 220 K under MAS at 8 kHz, yielding  $^{13}$ C enhancements in CarboPol of  $|\varepsilon_{13C}|$  > 2300 at 100 K. Owing to the long  $^{13}$ C  $T_1$  of the glassy OTP matrix, spontaneous  $^{13}$ C $-^{13}$ C spin diffusion can relay the  $^{13}$ C photo-CIDNP polarization far from the optically active molecules, resulting in bulk <sup>13</sup>C hyperpolarization, despite the low efficiency of spin diffusion for 13C spins at natural abundance. In the system investigated here, we determined that <sup>13</sup>C photo-CIDNP is most likely mediated by the threespin mixing mechanism, for which net polarization is generated. <sup>28,66-68</sup> These results represent an important step toward generalized signal enhancements in high-field NMR spectroscopy by optical hyperpolarization using photo-CIDNP of tailorable donor-acceptor molecular systems.

## ASSOCIATED CONTENT

## Supporting Information

The Supporting Information is available free of charge at https://pubs.acs.org/doi/10.1021/acs.jpclett.4c01121.

Synthetic methods and characterization of CarboPol, diagrams and pictures of the probe modifications used here, supplementary figures and tables, and a link to all of the raw NMR data (PDF).

## AUTHOR INFORMATION

#### **Corresponding Author**

Lyndon Emsley — Institut des Sciences et Ingenierie Chimiques, École Polytechnique Fedérale de Lausanne (EPFL), CH-1015 Lausanne, Switzerland; oorcid.org/0000-0003-1360-2572; Email: lyndon.emsley@epfl.ch

## **Authors**

- Federico De Biasi Institut des Sciences et Ingenierie Chimiques, École Polytechnique Fedérale de Lausanne (EPFL), CH-1015 Lausanne, Switzerland; orcid.org/ 0000-0001-6548-8383
- Michael A. Hope Institut des Sciences et Ingenierie Chimiques, École Polytechnique Fedérale de Lausanne (EPFL), CH-1015 Lausanne, Switzerland; Present Address: Department of Chemistry, University of Warwick, Gibbet Hill Road, Coventry CV4 7AL, United Kingdom; orcid.org/0000-0002-4742-9336
- Yunfan Qiu Department of Chemistry, Center for Molecular Quantum Transduction, Paula M. Trienens Institute for Sustainability and Energy, Northwestern University, Evanston, Illinois 60208-3113, United States; occid.org/0000-0002-4666-1424
- Paige J. Brown Department of Chemistry, Center for Molecular Quantum Transduction, Paula M. Trienens

- Institute for Sustainability and Energy, Northwestern University, Evanston, Illinois 60208-3113, United States; orcid.org/0000-0002-2934-0098
- Máté Visegrádi Institut des Sciences et Ingenierie Chimiques, École Polytechnique Fedérale de Lausanne (EPFL), CH-1015 Lausanne, Switzerland
- Olivier Ouari Aix-Marseille University, Centre National de la Recherche Scientifique (CNRS), Institut de Chimie Radicalaire, 13013 Marseille, France; orcid.org/0000-0003-4320-4313
- Michael R. Wasielewski Department of Chemistry, Center for Molecular Quantum Transduction, Paula M. Trienens Institute for Sustainability and Energy, Northwestern University, Evanston, Illinois 60208-3113, United States; orcid.org/0000-0003-2920-5440

Complete contact information is available at: https://pubs.acs.org/10.1021/acs.jpclett.4c01121

#### **Notes**

The authors declare no competing financial interest.

### ACKNOWLEDGMENTS

This work has been supported by the Swiss National Science Foundation Grant 200020\_212046 and the European Union's Horizon 2020 Research and Innovation Programme under Grant Agreement 101008500 (PANACEA). This research was also supported as part of the Center for Molecular Quantum Transduction, an Energy Frontier Research Center funded by the U.S. Department of Energy (DOE), Office of Science, Basic Energy Sciences (BES), under Award DE-SC0021314 (to Yunfan Qiu and Michael R. Wasielewski, for preparation and characterization of CarboPol).

#### REFERENCES

- (1) Abragam, A. The Principles of Nuclear Magnetism, 1st ed.; Clarendon Press: Oxford, U.K., 1961.
- (2) Lilly Thankamony, A. S.; Wittmann, J. J.; Kaushik, M.; Corzilius, B. Dynamic nuclear polarization for sensitivity enhancement in modern solid-state NMR. *Prog. Nucl. Magn. Reson. Spectrosc.* **2017**, 102–103, 120–195.
- (3) Eills, J.; Budker, D.; Cavagnero, S.; Chekmenev, E. Y.; Elliott, S. J.; Jannin, S.; Lesage, A.; Matysik, J.; Meersmann, T.; Prisner, T.; Reimer, J. A.; Yang, H.; Koptyug, I. V. Spin Hyperpolarization in Modern Magnetic Resonance. *Chem. Rev.* **2023**, *123* (4), 1417–1551.
- (4) Griesinger, C.; Bennati, M.; Vieth, H. M.; Luchinat, C.; Parigi, G.; Höfer, P.; Engelke, F.; Glaser, S. J.; Denysenkov, V.; Prisner, T. F. Dynamic nuclear polarization at high magnetic fields in liquids. *Prog. Nucl. Magn. Reson. Spectrosc.* **2012**, *64*, 4–28.
- (5) Barnes, A. B.; De Paepe, G.; van der Wel, P. C. A.; Hu, K.-N.; Joo, C.-G.; Bajaj, V. S.; Mak-Jurkauskas, M. L.; Sirigiri, J. R.; Herzfeld, J.; Temkin, R. J.; Griffin, R. G. High-Field Dynamic Nuclear Polarization for Solid and Solution Biological NMR. *Appl. Magn. Reson.* **2008**, 34 (3–4), 237–263.
- (6) Bowers, C. R.; Weitekamp, D. P. Transformation of Symmetrization Order to Nuclear-Spin Magnetization by Chemical Reaction and Nuclear Magnetic Resonance. *Phys. Rev. Lett.* **1986**, *57* (21), 2645–2648.
- (7) Pravica, M. G.; Weitekamp, D. P. Net NMR alignment by adiabatic transport of parahydrogen addition products to high magnetic field. *Chem. Phys. Lett.* **1988**, *145* (4), 255–258.
- (8) Adams, R. W.; Aguilar, J. A.; Atkinson, K. D.; Cowley, M. J.; Elliott, P. I. P.; Duckett, S. B.; Green, G. G. R.; Khazal, I. G.; López-Serrano, J. n.; Williamson, D. C. Reversible Interactions with para-Hydrogen Enhance NMR Sensitivity by Polarization Transfer. *Science* **2009**, 323 (5922), 1708–1711.

- (9) Ardenkjær-Larsen, J. H.; Fridlund, B.; Gram, A.; Hansson, G.; Hansson, L.; Lerche, M. H.; Servin, R.; Thaning, M.; Golman, K. Increase in signal-to-noise ratio of > 10,000 times in liquid-state NMR. *Proc. Natl. Acad. Sci. U.S.A.* 2003, 100 (18), 10158–10163.
- (10) Ardenkjaer-Larsen, J.-H.; Boebinger, G. S.; Comment, A.; Duckett, S.; Edison, A. S.; Engelke, F.; Griesinger, C.; Griffin, R. G.; Hilty, C.; Maeda, H.; Parigi, G.; Prisner, T.; Ravera, E.; van Bentum, J.; Vega, S.; Webb, A.; Luchinat, C.; Schwalbe, H.; Frydman, L. Facing and Overcoming Sensitivity Challenges in Biomolecular NMR Spectroscopy. *Angew. Chem., Int. Ed.* 2015, 54 (32), 9162–9185.
- (11) Ni, Q. Z.; Daviso, E.; Can, T. V.; Markhasin, E.; Jawla, S. K.; Swager, T. M.; Temkin, R. J.; Herzfeld, J.; Griffin, R. G. High Frequency Dynamic Nuclear Polarization. *Acc. Chem. Res.* **2013**, 46 (9), 1933–1941.
- (12) Maly, T.; Debelouchina, G. T.; Bajaj, V. S.; Hu, K.-N.; Joo, C.-G.; Mak-Jurkauskas, M. L.; Sirigiri, J. R.; van der Wel, P. C. A.; Herzfeld, J.; Temkin, R. J.; Griffin, R. G. Dynamic nuclear polarization at high magnetic fields. *J. Chem. Phys.* **2008**, *128* (5), 052211.
- (13) Lesage, A.; Lelli, M.; Gajan, D.; Caporini, M. A.; Vitzthum, V.; Miéville, P.; Alauzun, J.; Roussey, A.; Thieuleux, C.; Mehdi, A.; Bodenhausen, G.; Coperet, C.; Emsley, L. Surface Enhanced NMR Spectroscopy by Dynamic Nuclear Polarization. *J. Am. Chem. Soc.* **2010**, *132* (44), 15459–15461.
- (14) Rossini, A. J.; Zagdoun, A.; Hegner, F.; Schwarzwälder, M.; Gajan, D.; Copéret, C.; Lesage, A.; Emsley, L. Dynamic Nuclear Polarization NMR Spectroscopy of Microcrystalline Solids. *J. Am. Chem. Soc.* **2012**, *134* (40), 16899–16908.
- (15) Tycko, R.; Pines, A.; Stehlik, D. Time-resolved optical nuclear polarization by rapid field switching. *Chem. Phys. Lett.* **1982**, 93 (4), 392–395.
- (16) Hausser, K. H.; Wolf, H. C. Optical Spin Polarization in Molecular Crystals. In Advances in Magnetic and Optical Resonance, Academic Press 1976, 8, 85–121.
- (17) Stehlik, D.; Doehring, A.; Colpa, J. P.; Callaghan, E.; Kesmarky, S. Optical nuclear polarization in molecular crystals through an optical excitation cycle. *Chem. Phys.* **1975**, *7* (2), 165–186.
- (18) Eichhorn, T. R.; Parker, A. J.; Josten, F.; Muller, C.; Scheuer, J.; Steiner, J. M.; Gierse, M.; Handwerker, J.; Keim, M.; Lucas, S.; Qureshi, M. U.; Marshall, A.; Salhov, A.; Quan, Y.; Binder, J.; Jahnke, K. D.; Neumann, P.; Knecht, S.; Blanchard, J. W.; Plenio, M. B.; Jelezko, F.; Emsley, L.; Vassiliou, C. C.; Hautle, P.; Schwartz, I. Hyperpolarized Solution-State NMR Spectroscopy with Optically Polarized Crystals. J. Am. Chem. Soc. 2022, 144 (6), 2511–2519.
- (19) Eichhorn, T. R.; Haag, M.; van den Brandt, B.; Hautle, P.; Wenckebach, W. T. High proton spin polarization with DNP using the triplet state of pentacene. *Chem. Phys. Lett.* **2013**, 555, 296–299. (20) Tateishi, K.; Negoro, M.; Nishida, S.; Kagawa, A.; Morita, Y.;
- Kitagawa, M. Room temperature hyperpolarization of nuclear spins in bulk. *Proc. Natl. Acad. Sci. U.S.A.* **2014**, *111* (21), 7527–7530. (21) Kaptein, R.; Dijkstra, K.; Nicolay, K. Laser photo-CIDNP as a
- surface probe for proteins in solution. *Nature* **1978**, 274 (5668), 293–294.
- (22) Goez, M. Photo-CIDNP Spectroscopy. In Annual Reports on NMR Spectroscopy, Academic Press 2009, 66, 77–147.
- (23) Ward, H. R.; Lawler, R. G. Nuclear magnetic resonance emission and enhanced absorption in rapid organometallic reactions. *J. Am. Chem. Soc.* **1967**, 89 (21), 5518–5519.
- (24) Bargon, J.; Fischer, H.; Johnsen, U. Kernresonanz-Emissionslinien während rascher Radikalreaktionen. *Z. Naturforsch. A* **1967**, 22 (10), 1551–1555.
- (25) Kaptein, R. Chemically induced dynamic nuclear polarization in five alkyl radicals. *Chem. Phys. Lett.* **1968**, 2 (4), 261–267.
- (26) Matysik, J.; Ding, Y.; Kim, Y.; Kurle, P.; Yurkovskaya, A.; Ivanov, K.; Alia, A. Photo-CIDNP in Solid State. *Appl. Magn. Reson.* **2022**, 53 (3–5), 521–537.
- (27) Sosnovsky, D. V.; Jeschke, G.; Matysik, J.; Vieth, H.-M.; Ivanov, K. L. Level crossing analysis of chemically induced dynamic nuclear polarization: Towards a common description of liquid-state and solid-state cases. *J. Chem. Phys.* **2016**, *144* (14), No. 144202.

- (28) Sosnovsky, D. V.; Lukzen, N. N.; Vieth, H.-M.; Jeschke, G.; Gräsing, D.; Bielytskyi, P.; Matysik, J.; Ivanov, K. L. Magnetic field and orientation dependence of solid-state CIDNP. *J. Chem. Phys.* **2019**, *150* (9), No. 094105.
- (29) Zysmilich, M. G.; McDermott, A. Photochemically Induced Dynamic Nuclear Polarization in the Solid-State <sup>15</sup>N Spectra of Reaction Centers from Photosynthetic Bacteria Rhodobacter sphaeroides R-26. *J. Am. Chem. Soc.* **1994**, *116* (18), 8362–8363.
- (30) McDermott, A.; Zysmilich, M. n. G.; Polenova, T. Solid state NMR studies of photoinduced polarization in photosynthetic reaction centers: mechanism and simulations. *Solid State Nucl. Magn. Reson.* **1998**, *11* (1–2), 21–47.
- (31) Daviso, E.; Janssen, G. J.; Alia, A.; Jeschke, G.; Matysik, J.; Tessari, M. A 10 000-fold Nuclear Hyperpolarization of a Membrane Protein in the Liquid Phase via a Solid-State Mechanism. *J. Am. Chem. Soc.* **2011**, *133* (42), 16754–16757.
- (32) Daviso, E.; Jeschke, G.; Matysik, J. Photochemically Induced Dynamic Nuclear Polarization (Photo-CIDNP) Magic-Angle Spinning NMR. In Biophysical Techniques in Photosynthesis, Springer, Dordrecht 2008, 26, 385–399.
- (33) Zysmilich, M. G.; McDermott, A. Photochemically Induced Nuclear Spin Polarization in Bacterial Photosynthetic Reaction Centers: Assignments of the <sup>15</sup>N SSNMR Spectra. *J. Am. Chem. Soc.* **1996**, *118* (25), 5867–5873.
- (34) Matysik, J.; Alia; Gast, P.; van Gorkom, H. J.; Hoff, A. J.; de Groot, H. J. M. Photochemically induced nuclear spin polarization in reaction centers of photosystem II observed by  $^{13}$ C-solid-state NMR reveals a strongly asymmetric electronic structure of the  $P_{680.}$ + primary donor chlorophyll. *Proc. Natl. Acad. Sci. U.S.A.* **2000**, 97 (18), 9865–9870.
- (35) Zysmilich, M. G.; McDermott, A. Natural abundance solid-state carbon NMR studies of photosynthetic reaction centers with photoinduced polarization. *Proc. Natl. Acad. Sci. U.S.A.* **1996**, 93 (14), 6857–6860.
- (36) Surendran Thamarath, S.; Alia, A.; Roy, E.; Sai Sankar Gupta, K. B.; Golbeck, J. H.; Matysik, J. The field-dependence of the solid-state photo-CIDNP effect in two states of heliobacterial reaction centers. *Photosynth. Res.* **2013**, *117* (1–3), 461–469.
- (37) Matysik, J.; Alia; Gast, P.; Lugtenburg, J.; Hoff, A. J.; de Groot, H. J. M. Photochemically induced dynamic nuclear polarization in bacterial photosynthetic reaction centres observed by <sup>13</sup>C solid-state NMR. In *Perspectives on Solid State NMR in Biology*; Kiihne, S. R., de Groot, H. J. M., Eds.; Springer: Dordrecht, Netherlands, 2001; Focus on Structural Biology, Vol. 1, pp 215–225, DOI: 10.1007/978-94-017-2579-8 19.
- (38) Daviso, E.; Prakash, S.; Alia, A.; Gast, P.; Neugebauer, J.; Jeschke, G.; Matysik, J. The electronic structure of the primary electron donor of reaction centers of purple bacteria at atomic resolution as observed by photo-CIDNP <sup>13</sup>C NMR. *Proc. Natl. Acad. Sci. U.S.A.* **2009**, *106* (52), 22281–22286.
- (39) Alia; Roy, E.; Gast, P.; van Gorkom, H. J.; de Groot, H. J. M.; Jeschke, G.; Matysik, J. Photochemically Induced Dynamic Nuclear Polarization in Photosystem I of Plants Observed by <sup>13</sup>C Magic-Angle Spinning NMR. *J. Am. Chem. Soc.* **2004**, *126* (40), 12819–12826.
- (40) Prakash, S.; Alia; Gast, P.; de Groot, H. J. M.; Jeschke, G.; Matysik, J. Magnetic Field Dependence of Photo-CIDNP MAS NMR on Photosynthetic Reaction Centers of Rhodobacter sphaeroides WT. *J. Am. Chem. Soc.* **2005**, *127* (41), *14290*–14298.
- (41) Polenova, T.; McDermott, A. E. A Coherent Mixing Mechanism Explains the Photoinduced Nuclear Polarization in Photosynthetic Reaction Centers. *J. Phys. Chem. B* **1999**, *103* (3), 535–548.
- (42) Diller, A.; Roy, E.; Gast, P.; van Gorkom, H. J.; de Groot, H. J. M.; Glaubitz, C.; Jeschke, G.; Matysik, J.; Alia, A. <sup>15</sup>N photochemically induced dynamic nuclear polarization magic-angle spinning NMR analysis of the electron donor of photosystem II. *Proc. Natl. Acad. Sci. U.S.A.* **2007**, *104* (31), 12767–12771.
- (43) Thamarath, S. S.; Heberle, J.; Hore, P. J.; Kottke, T.; Matysik, J. Solid-State Photo-CIDNP Effect Observed in Phototropin LOV1-

- C57S by <sup>13</sup>C Magic-Angle Spinning NMR Spectroscopy. *J. Am. Chem. Soc.* **2010**, *132* (44), 15542–15543.
- (44) Bielytskyi, P.; Gräsing, D.; Mote, K. R.; Sai Sankar Gupta, K. B.; Vega, S.; Madhu, P. K.; Alia, A.; Matysik, J.  $^{13}$ C  $\rightarrow$   $^{1}$ H transfer of light-induced hyperpolarization allows for selective detection of protons in frozen photosynthetic reaction center. *J. Magn. Reson.* **2018**, 293, 82–91.
- (45) De Biasi, F.; Hope, M. A.; Avalos, C. E.; Karthikeyan, G.; Casano, G.; Mishra, A.; Badoni, S.; Stevanato, G.; Kubicki, D. J.; Milani, J.; Ansermet, J.-P.; Rossini, A. J.; Lelli, M.; Ouari, O.; Emsley, L. Optically Enhanced Solid-State <sup>1</sup>H NMR Spectroscopy. *J. Am. Chem. Soc.* **2023**, *145* (27), 14874–14883.
- (46) Colvin, M. T.; Carmieli, R.; Miura, T.; Richert, S.; Gardner, D. M.; Smeigh, A. L.; Dyar, S. M.; Conron, S. M.; Ratner, M. A.; Wasielewski, M. R. Electron Spin Polarization Transfer from Photogenerated Spin-Correlated Radical Pairs to a Stable Radical Observer Spin. J. Phys. Chem. A 2013, 117 (25), 5314–5325.
- (47) Mi, Q.; Ratner, M. A.; Wasielewski, M. R. Time-Resolved EPR Spectra of Spin-Correlated Radical Pairs: Spectral and Kinetic Modulation Resulting from Electron—Nuclear Hyperfine Interactions. *J. Phys. Chem. A* **2010**, *114* (1), 162–171.
- (48) Mi, Q.; Chernick, E. T.; McCamant, D. W.; Weiss, E. A.; Ratner, M. A.; Wasielewski, M. R. Spin Dynamics of Photogenerated Triradicals in Fixed Distance Electron Donor-Chromophore-Acceptor-TEMPO Molecules. J. Phys. Chem. A 2006, 110 (23), 7323-7333.
- (49) Hasharoni, K.; Levanon, H.; Greenfield, S. R.; Gosztola, D. J.; Svec, W. A.; Wasielewski, M. R. Radical Pair and Triplet State Dynamics of a Photosynthetic Reaction-Center Model Embedded in Isotropic Media and Liquid Crystals. *J. Am. Chem. Soc.* **1996**, *118* (42), 10228–10235.
- (50) Harvey, S. M.; Wasielewski, M. R. Photogenerated Spin-Correlated Radical Pairs: From Photosynthetic Energy Transduction to Quantum Information Science. *J. Am. Chem. Soc.* **2021**, *143* (38), 15508–15529.
- (51) Rugg, B. K.; Krzyaniak, M. D.; Phelan, B. T.; Ratner, M. A.; Young, R. M.; Wasielewski, M. R. Photodriven quantum teleportation of an electron spin state in a covalent donor—acceptor—radical system. *Nat. Chem.* **2019**, *11* (11), 981—986.
- (52) Qiu, Y.; Equbal, A.; Lin, C.; Huang, Y.; Brown, P. J.; Young, R. M.; Krzyaniak, M. D.; Wasielewski, M. R. Optical Spin Polarization of a Narrow-Linewidth Electron-Spin Qubit in a Chromophore/Stable-Radical System. *Angew. Chem., Int. Ed.* **2023**, 62 (6), No. e202214668.
- (53) Greenfield, S. R.; Svec, W. A.; Gosztola, D.; Wasielewski, M. R. Multistep Photochemical Charge Separation in Rod-like Molecules Based on Aromatic Imides and Diimides. *J. Am. Chem. Soc.* **1996**, *118* (28), 6767–6777.
- (54) Huang, Y.; Krzyaniak, M. D.; Young, R. M.; Wasielewski, M. R. Mechanistic Study of Electron Spin Polarization Transfer in Covalent Donor—Acceptor-Radical Systems. *Appl. Magn. Reson.* **2022**, *53* (7–9), 949–961.
- (55) Weiss, E. A.; Ratner, M. A.; Wasielewski, M. R. Direct Measurement of Singlet—Triplet Splitting within Rodlike Photogenerated Radical Ion Pairs Using Magnetic Field Effects: Estimation of the Electronic Coupling for Charge Recombination. *J. Phys. Chem. A* **2003**, *107* (19), 3639–3647.
- (56) Carmieli, R.; Mi, Q.; Ricks, A. B.; Giacobbe, E. M.; Mickley, S. M.; Wasielewski, M. R. Direct Measurement of Photoinduced Charge Separation Distances in Donor–Acceptor Systems for Artificial Photosynthesis Using OOP-ESEEM. J. Am. Chem. Soc. 2009, 131 (24), 8372–8373.
- (57) Lelli, M.; Chaudhari, S. R.; Gajan, D.; Casano, G.; Rossini, A. J.; Ouari, O.; Tordo, P.; Lesage, A.; Emsley, L. Solid-State Dynamic Nuclear Polarization at 9.4 and 18.8 T from 100 K to Room Temperature. J. Am. Chem. Soc. 2015, 137 (46), 14558–14561.
- (58) Earle, K. A.; Moscicki, J. K.; Polimeno, A.; Freed, J. H. A 250 GHz ESR study of o-terphenyl: Dynamic cage effects above T<sub>c</sub>. J. Chem. Phys. **1997**, 106 (24), 9996–10015.

- (59) Andreozzi, L.; Cianflone, F.; Donati, C.; Leporini, D. Jump reorientation of a molecular probe in the glass transition region of oterphenyl. *J. Phys.: Condens. Matter* **1996**, *8* (21), 3795–3809.
- (60) Savitsky, A.; Plato, M.; Möbius, K. The Temperature Dependence of Nitroxide Spin-Label Interaction Parameters: a High-Field EPR Study of Intramolecular Motional Contributions. *Appl. Magn. Reson.* **2010**, *37* (1–4), 415–434.
- (61) Ernst, R. R.; Anderson, W. A. Application of Fourier Transform Spectroscopy to Magnetic Resonance. *Rev. Sci. Instrum.* **1966**, 37 (1), 93–102.
- (62) Björgvinsdóttir, S.; Walder, B. J.; Pinon, A. C.; Emsley, L. Bulk Nuclear Hyperpolarization of Inorganic Solids by Relay from the Surface. *J. Am. Chem. Soc.* **2018**, *140* (25), 7946–7951.
- (63) Halse, M. E.; Zagdoun, A.; Dumez, J.-N.; Emsley, L. Macroscopic nuclear spin diffusion constants of rotating polycrystal-line solids from first-principles simulation. *J. Magn. Reson.* **2015**, 254, 48–55.
- (64) Prisco, N. A.; Pinon, A. C.; Emsley, L.; Chmelka, B. F. Scaling analyses for hyperpolarization transfer across a spin-diffusion barrier and into bulk solid media. *Phys. Chem. Chem. Phys.* **2021**, 23 (2), 1006–1020.
- (65) Goldstein, R. A.; Boxer, S. G. Effects of Nuclear Spin Polarization on Reaction Dynamics in Photosynthetic Bacterial Reaction Centers. *Biophys. J.* **1987**, *51* (6), 937–946.
- (66) Jeschke, G. A New Mechanism for Chemically Induced Dynamic Nuclear Polarization in the Solid State. *J. Am. Chem. Soc.* **1998**, 120 (18), 4425–4429.
- (67) Jeschke, G. Electron-electron-nuclear three-spin mixing in spin-correlated radical pairs. *J. Chem. Phys.* **1997**, *106* (24), 10072–10086.
- (68) Jeschke, G.; Matysik, J. A reassessment of the origin of photochemically induced dynamic nuclear polarization effects in solids. *Chem. Phys.* **2003**, 294 (3), 239–255.